

INVITED PAPER

PACS numbers: 42.55.Lt; 32.30.-r; 52.20.Hv
DOI: 10.1070/QE2004v034n03ABEH002609

Deactivation of the 6*s* and 6*s*′ states of a xenon atom in collisions with helium, argon, and xenon atoms

L.V. Semenova, N.N. Ustinovskii, I.V. Kholin

***Abstract*. A series of publications devoted to the study of collisional deactivation of Xe atoms in the 6*s* and 6*s*′ states in high-pressure Ar – He and He – Xe mixtures with a low content of Xe is summarised. The processes of quenching of the $^1P_1$, $^3P_0$, $^3P_1$, and $^3P_2$ levels are studied in two-particle $Xe^* + Ar(He) \rightarrow$ products + Ar(He), three-particle $Xe^* + 2Ar(2He) \rightarrow ArXe^*(HeXe^*) + Ar(He)$, and three-particle $Xe^* + Xe + Ar(He) \rightarrow Xe_2^* + Ar(He)$ collisions. The gases were excited by a fast-electron beam. The measurements were performed by the method of absorption probing by analysing the time dependence of the concentration of the excited states in the afterglow of the electron beam. The rate constants of 24 plasma-chemical reactions were measured, 17 of which – for the first time.**

Keywords: *xenon, collisional deactivation, rare-gas lasers, high-pressure lasers.*

1. Introduction

The paper is devoted to the experimental study of deactivation of excited xenon atoms in the 6*s* and 6*s*′ states in collisions with ground-state atoms of argon, helium, and xenon itself. The two- and three-particle plasma-chemical reactions were studied which dominate in gas mixtures with low relative concentrations of xenon. These studies are both of fundamental and practical importance, in particular, for a new, rapidly developing class of high-power high-pressure near-IR rare-gas mixture lasers (see review [1]).

The intense development of UV excimer lasers gave an impetus to the studies of various plasma-chemical processes in high-pressure mixtures of rare gases in the early 1970s [2, 3]. Analysis of the literature shows, however, that many of these reactions have not been adequately studied so far. For this reason, attempts to describe quantitatively kinetic processes proceeding in lasers on the $5d - 6p$ transitions in a Xe atom [4 – 6] (the most promising of all high-pressure rare-gas lasers) ran into requirements to have more accurate experimental data on the rate constants of elementary plasma-chemical processes, in particular, reactions of collisional quenching of the lower excited states of a Xe atom in the Ar – Xe, He – Xe, and He – Ar – Xe gas mixtures, which are used as active media in these lasers [1, 7 – 13].

The matter is that these reactions, which determine the populations of the 6*s* and 6*s*′ states, considerably affect the total laser kinetics. Thus, upon electroionisation excitation of the most interesting Ar – Xe mixtures, the laser transitions in Xe are pumped not from the ground state but from these excited states produced in the active medium by a fast-electron beam [1]. It is this mechanism (see also Ref. [14]) that determines the high efficiency of the Ar – Xe lasers. In addition, because the 6*s* and 6*s*′ states are coupled with the 6*p* states of a Xe atom, belonging to the manifold of the lower laser levels, by rapid electron mixing reactions proceeding via the allowed transitions of the type

$$Xe(6s,\ 6s') + e \leftrightarrow Xe(6p) + e, \tag{1}$$

while the resonance $6s'[1/2]_1^o(^1P_1)$ level is also involved to rapid collision reactions of the type

$$Xe(6s'[1/2]_1^o) + Ar \leftrightarrow Xe(6p[1/2]_1) + Ar, \tag{2}$$

(see, for example, Ref. [15]), the processes of collisional deactivation prove to be one of the main channels of the depletion of lower laser levels during the pump pulse.

For all these reasons, these studies were initiated at the Department of Quantum Radiophysics headed by academician N.G. Basov at the P.N. Lebedev Physics Institute, Russian Academy of Sciences (see also Refs [16 – 19]). Experiments were performed on the Tandem laser setup [1] by exciting various Ar – Xe and He – Xe gas media by a fast-electron beam. The rate constants of 24 plasma-chemical reactions [(3) – (26) in Tables 1 and 2] were measured by the method of absorption probing by analysing the time dependence of the concentration of the excited states.

2. Studies of collisional quenching in xenon mixtures

The first measurements of the rate constants of collisional quenching of excited Xe atoms in the high-pressure He – Xe and Ar – Xe mixtures of interest to us were performed in paper [20]. The mixtures with the partial pressures of xenon between 260 and 2580 Torr and the buffer gas pressures from zero to 1.95×10^4 Torr were excited by a relativistic electron beam with the pulse duration of 2 ns. The time dependence of VUV luminescence was studied at a wave-

L.V. Semenova, N.N. Ustinovskii, I.V. Kholin P.N. Lebedev Physics Institute, Russian Academy of Sciences, Leninskii prosp. 53, 119991 Moscow, Russia

Received 12 May 2003
Kvantovaya Elektronika **34** (3) 189 – 198 (2004)
Translated by M.N. Sapozhnikov

Table 1. Rate constants of collisional deactivation of the 6*s* levels of a xenon atom in the Ar–Xe mixture.

Reaction	Rate constant*	References	Reaction number
$Xe(6s'[1/2]_1^o)^1P_1 + Xe + Ar \rightarrow Xe_2^* + Ar$	7×10^{-32}	[30]	(3)
	8.3×10^{-32}	[31]	
	$(3.6 \pm 0.3) \times 10^{-32}$	This paper	
$Xe(6s'[1/2]_0^o)^3P_0 + Xe + Ar \rightarrow Xe_2^* + Ar$	$(3.2 \pm 0.3) \times 10^{-32}$	This paper	(4)
$Xe(6s[3/2]_1^o)^3P_1 + Xe + Ar \rightarrow Xe_2^* + Ar$	$(2.1 \pm 0.2) \times 10^{-31}$	[21]	(5)
	4.5×10^{-32}	[31]	
	$(8.6 \pm 0.4) \times 10^{-32}$	[33]	
	$(2.8 \pm 0.9) \times 10^{-32}$	This paper	
$Xe(6s[3/2]_2^o)^3P_2 + Xe + Ar \rightarrow Xe_2^* + Ar$	2.3×10^{-32}	[20]	(6)
	$(2.15 \pm 0.25) \times 10^{-32}$	[21]	
	2.6×10^{-32}	[31]	
	$(1.5 \pm 0.2) \times 10^{-31}$	[33]	
	$(1.8 \pm 0.6) \times 10^{-32}$	This paper	
$Xe(6s'[1/2]_1^o)^1P_1 + 2Ar \rightarrow ArXe^* + Ar$	$< 10^{-35}$	This paper	(7)
$Xe(6s'[1/2]_0^o)^3P_0 + 2Ar \rightarrow ArXe^* + Ar$	$< 10^{-35}$	This paper	(8)
$Xe(6s[3/2]_1^o)^3P_1 + 2Ar \rightarrow ArXe^* + Ar$	$< 10^{-35}$	This paper	(9)
$Xe(6s[3/2]_1^o)^3P_2 + 2Ar \rightarrow ArXe^* + Ar$	$(3 \pm 3) \times 10^{-34}$	[23]	(10)
	$< 10^{-35}$	This paper	
$Xe(6s'[1/2]_1^o)^1P_1 + Ar \rightarrow Xe(6s',\ 6s) + Ar$	$(8.5 \pm 5.0) \times 10^{-12}$	[15]	(11)
	$(1.5 \pm 0.5) \times 10^{-12}$	[32]	
	$< 2.1 \times 10^{-14}$	[17]	
	$(1.5 \pm 0.3) \times 10^{-14}$	This paper	
$Xe(6s'[1/2]_0^o)^3P_0 + Ar \rightarrow Xe(6s',\ 6s) + Ar$	$\sim 5 \times 10^{-14}$	[15]	(12)
	$(3.6 \pm 0.8) \times 10^{-15}$	[32]	
	$< 9.7 \times 10^{-15}$	[17]	
	$(8.1 \pm 0.9) \times 10^{-15}$	This paper	
$Xe(6s[3/2]_1^o)^3P_1 + Ar \rightarrow Xe(6s) + Ar$	$(1.5 \pm 0.3) \times 10^{-14}$	[21]	(13)
	1.7×10^{-14}	[22]	
	3.0×10^{-14}	[31]	
	$(4.0 \pm 0.5) \times 10^{-13}$	[32]	
	$< 9 \times 10^{-15}$	[16]	
	$(3.2 \pm 1.5) \times 10^{-15}$	This paper	
$Xe(6s[3/2]_2^o)^3P_2 + Ar \rightarrow Xe(6s) + Ar$	$(8.3 \pm 1.5) \times 10^{-17}$	[21]	(14)
	$(5.0 \pm 0.7) \times 10^{-16}$	[23]	
	$(7.3 \pm 0.9) \times 10^{-16}$	[33]	
	$< 2.5 \times 10^{-15}$	[16]	
	$(5.0 \pm 0.6) \times 10^{-16}$	This paper	

Note: *Rate constants of reactions (3)–(10) and (11)–(14) are measured in $cm^6\ s^{-1}$ and $cm^3\ s^{-1}$, respectively.

Table 2. Rate constants of collisional deactivation of the 6*s* levels of a xenon atom in the He–Xe mixture.

Reaction	Rate constant*	References	Reaction number
$Xe(6s'[1/2]_1^o)^1P_1 + Xe + He \rightarrow Xe_2^* + He$	$(2.5 \pm 0.3) \times 10^{-32}$	This paper	(15)
$Xe(6s'[1/2]_0^o)^3P_0 + Xe + He \rightarrow Xe_2^* + He$	$(2.2 \pm 0.2) \times 10^{-32}$	This paper	(16)
$Xe(6s[3/2]_1^o)^3P_1 + Xe + He \rightarrow Xe_2^* + He$	$(2.1 \pm 0.2) \times 10^{-32}$	This paper	(17)
$Xe(6s[3/2]_2^o)^3P_2 + Xe + He \rightarrow Xe_2^* + He$	1.4×10^{-32}	[20]	(18)
	$(1.7 \pm 0.2) \times 10^{-32}$	This paper	
$Xe(6s'[1/2]_1^o)^1P_1 + 2He \rightarrow HeXe^* + He$	$< 2 \times 10^{-35}$	This paper	(19)
$Xe(6s'[1/2]_0^o)^3P_0 + 2He \rightarrow HeXe^* + He$	$< 2 \times 10^{-35}$	This paper	(20)
$Xe(6s[3/2]_1^o)^3P_1 + 2He \rightarrow HeXe^* + He$	$< 10^{-35}$	This paper	(21)
$Xe(6s[3/2]_2^o)^3P_2 + 2He \rightarrow HeXe^* + He$	$< 2 \times 10^{-35}$	This paper	(22)
$Xe(6s'[1/2]_1^o)^1P_1 + He \rightarrow Xe(6s',\ 6s) + He$	$\sim 1.2 \times 10^{-13}$	[15]	(23)
	$< 3 \times 10^{-15}$	This paper	
$Xe(6s'[1/2]_0^o)^3P_0 + He \rightarrow Xe(6s',\ 6s) + He$	$\sim 5 \times 10^{-13}$	[15]	(24)
	$< 2.5 \times 10^{-15}$	This paper	
$Xe(6s[3/2]_1^o)^3P_1 + He \rightarrow Xe(6s) + He$	$< 3 \times 10^{-15}$	This paper	(25)
$Xe(6s[3/2]_2^o)^3P_2 + He \rightarrow Xe(6s) + He$	$< 10^{-15}$	This paper	(26)

Note: * Rate constants of reactions (15)–(22) and (23)–(26) are measured in $cm^6\ s^{-1}$ and $cm^3\ s^{-1}$, respectively.

length of 173 nm corresponding to transitions from the lower vibrational levels of the $Xe_2^*(^{1,3}\Sigma_u^+)$ excimer states to the ground $Xe_2^*(^1\Sigma_g)$ state (the so-called second emission continuum of rare gases). The luminescence signal was bell-shaped, with a steep leading edge and a less steep trailing edge. The time dependence of the leading edge was quite accurately described by the exponential dependence with the exponent

$$1/\tau = \{k_1[\mathrm{Xe}] + k_2[\mathrm{Ar}]\ (\text{or } [\mathrm{He}])\}\ [\mathrm{Xe}], \tag{27}$$

where the constants k_1 and k_2 obtained in the experiment were interpreted as the rate constants of excitation energy transfer from Xe^* to the Xe_2^* excimer in the reaction

$$Xe^* + 2Xe \rightarrow Xe_2^* + Xe \tag{28}$$

and reactions

$$Xe^* + Xe + Ar(He) \rightarrow Xe_2^* + Ar(He) \tag{29}$$

studied in our paper. Because relaxation flows from different 6*s* states of the Xe atom (see Fig. 1) were not separated in the experiment, it seems reasonable to assign the experimental values of k_2 equal to 2.3×10^{-32} and 1.4×10^{-32} cm^6 s^{-1} to the slowest reactions in the given group [reactions (6) and (18) in Tables 1 and 2].

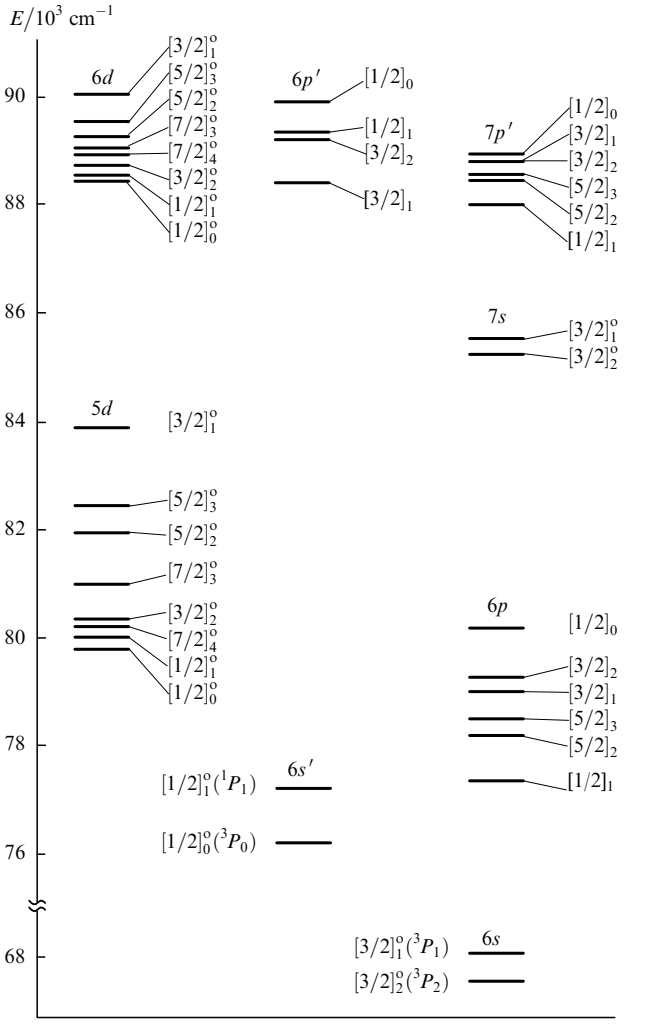

Figure 1. Energy level diagram of a xenon atom.

A similar method of measurements using excitation by an electron beam was employed in Ref. [21]. The Ar–Xe mixtures were studied in which the Xe concentration was varied from 8.4×10^{13} to 2.67×10^{17} cm^{-3} and the Ar concentration was varied from 5.1×10^{19} to 2.9×10^{20} cm^{-3}. The time dependence of VUV luminescence was detected at $\sim$ 147 nm (the first emission continuum) and $\sim$ 173 nm (the second continuum). The luminescence decay at 147 nm exhibited the fast and slow components, the slow component being identical to the luminescence decay at $\sim$ 173 nm. The fast component was assigned to transitions from the upper vibrational levels of the $Xe_2^*(^1\Sigma_u^+)$ state, which correlates with the $^3P_1$ state of the Xe atom (resonance emission at the atomic $^3P_1 - {}^1S_0$ transition of xenon was assumed trapped), while the slow component was assigned to energy transfer from the metastable $^3P_2$ level. Analysis of the experimental dependences of the decay rates on the concentrations of Ar and Xe gave the values 2.1×10^{-31} and 2.15×10^{-32} cm^6 s^{-1} for the rate constants of three-particle reactions (5) and (6), respectively, and 1.5×10^{-14} and 8.3×10^{-17} cm ^{3}s^{-1} for the rate constants of two-particle reactions (13) and (14), respectively.

Reaction (13) was also studied in Ref. [13], where the resonance $^3P_1$ state of the Xe atom was selectively excited by VUV radiation from a xenon lamp at 147 nm. The luminescence intensity at the 173-nm emission wavelength of the Xe_2^* excimer was studied. Mixtures with the partial pressure of xenon of a few Torr at the argon pressure up to 10^3 Torr were investigated. It was assumed that the rate of reaction (5) is low and the observed deactivation rates are completely determined by reaction (13) with the rate constant equal to 1.7×10^{-14} cm^3 s^{-1}.

In Ref. [23], kinetic processes in the Ar–Xe mixtures were studied by the method of absorption probing. The total pressure did not exceed a few Torr. The measurements were performed in the gas-mixture flow moving at the known velocity and excited with a glow electric discharge at the entry to a measurement chamber. The time dependence of the concentration of the Xe($^3P_2$) metastable state was detected by a decrease in the absorption coefficient of probe radiation (at one of the $6p - 6s$ transitions corresponding to this state) with removing the gas flow from the excitation source. By analysing the experimental time dependences obtained this way, the authors [23] determined the rate constants of two- and three-particle quenching of the Xe($^3P_2$) state by Ar atoms. The rate constants for reactions (10) and (14) were 3×10^{-34} cm^6 s^{-1} and 5.0×10^{-16} cm^3 s^{-1}, respectively.

Note that kinetic processes in the active media of IR lasers on the transitions in Xe (see, for example, Refs [5, 24, 25]) and UV excimer lasers (for example, Refs [26, 27]) were often analysed by using for reaction (10) the rate constants presented in monograph [2] and equal to 10^{-33} cm^6 s^{-1} (presented in Ref. [2] as taken from Ref. [28]) and 7×10^{-34} cm^6 s^{-1} (taken from Ref. [29]). The use of such evidently overstated values is a pure misunderstanding because the authors [28] finally reported in Ref. [23] the value of the rate constant that was three times lower, whereas reaction (10) was not discussed in Ref. [29] at all.

In Ref. [15] devoted to the study of collisional deactivation of the 6*p* levels of Xe atoms, the data on quenching of

the $6s'$ levels in two-particle collisions with Ar and He were also obtained. A tunable dye laser was used to excite the $6p$ levels due to two-photon absorption. The time dependence of IR luminescence corresponding to the relevant $6p-6s$ transitions was detected in experiments. The population dynamics of the $6s'$ states was analysed indirectly using an adequate kinetic model, where the rate constants 8.5×10^{-12}, 5×10^{-14}, 1.2×10^{-13}, and 5×10^{-13} cm^3 s^{-1} for reactions (11), (12), (23), and (24), respectively, were the approximation parameters.

Processes of deactivation in the Ar–Xe mixtures were studied in Refs [30, 31]. Gases were excited by an alpha-particle beam. The dynamics of broadband excimer emission of xenon in the second continuum and of emission at atomic transitions from the resonance $^1P_1$ and $^3P_1$ levels to the ground state at 129.6 and 147.0 nm, respectively, was studied in Ref. [31]. The IR emission dynamics of atomic xenon at two intermultiplet $6p-6s$ transitions at 826 and 980 nm was analysed in Ref. [30]. The rate constants measured for reactions (5) and (6) were 4.5×10^{-32} and 2.6×10^{-32} cm^6 s^{-1}, respectively [31], and $(7-8)\times10^{-32}$ cm^6 s^{-1} for reaction (3) [30, 31].

The resonance $^3P_1$ and $^1P_1$ states of the Xe atom were excited in Ref. [32] by short pulses of monochromatic synchrotron radiation. The Ar–Xe mixtures were studied with a rather low relative concentration of Xe, at the level of 1 ppm, and at extremely high total pressures (14–71 atm). It was assumed that, under such conditions, collisions with Xe atoms are negligible and the collisional deactivation of Xe* occurs due to two- and three-particle collisions with buffer gas atoms. The time dependence of broadband emission at ~130 and 147.9 nm was studied, which was interpreted by the authors as emission of heteronuclear complexes formed from Ar and Xe* upon their van der Waals interaction. The decays of both spectral components exhibited the fast and slow components. A computer kinetic model describing deactivation processes was constructed. The numerical fit of the experimental data gave the rate constants equal to 1.5×10^{-12} and 4.0×10^{-13} cm^3 s^{-1} for reactions (11) and (13), respectively (these values being probably related to the fast components of the measured emission decay), and to 3.6×10^{-15} cm^3 s^{-1} for reaction (12) (the value corresponding to the slow component).

In the last paper [33] considered in this section, the resonance $^3P_1$ states of Xe and Kr atoms also were excited selectively by short light pulses from a dye laser upon three-photon absorption. The Ar–Kr, Kr–Xe, and Ar–Xe mixtures were studied at the total pressure up to 1000 Torr and the partial pressure of the working gas of several tens of Torr. The time dependence of VUV luminescence from the excited resonance level in mixtures with Xe at 147 nm was investigated. The decay of VUV luminescence was described by a sum of two exponentials corresponding, according to the interpretation of the authors, to the deactivation of the $^3P_1$ and $^3P_2$ states of xenon. The rate constants of reactions (5), (6), and (14) determined from the numerical fit of the experimental emission decays were 8.6×10^{-32} cm^6 s^{-1}, 1.5×10^{-31} cm^6 s^{-1}, and 7.3×10^{-16} cm^3 s^{-1}, respectively. At the same time, no contribution from two-particle reaction (13) to the deactivation of the $^3P_1$ level was observed within the accuracy of measurements.

3. Experimental setup

Experiments were performed on the Tandem laser setup [1]. We determined the rate constants of plasma-chemical reactions presented in Tables 1 and 2 by measuring the decay times of the $6s$ and $6s'$ states in the afterglow of a high-power fast-electron beam by the method of absorption probing. The absorption dynamics of the probe pulse at the wavelength of one of the $p-s$ transitions corresponding to the state under study was investigated. We measured the decay times of the $6s'[1/2]^o_1(^1P_1)$, $6s'[1/2]^o_0(^3P_0)$, $6s[3/2]^o_1(^3P_1)$ and $6s[3/2]^o_2(^3P_2)$ levels at seven transitions (see Fig. 1 and Table 3) with large oscillator strengths lying in the spectral range where the sensitivity of the photodetector was sufficiently high.

Table 3. Transitions in a xenon atom used in absorption experiments.

Xe transitions	λ/nm
$6p'[3/2]_1-6s'[1/2]^o_1$	893.1
$6p'[3/2]_2-6s'[1/2]^o_1$	834.7
$6p'[1/2]_1-6s'[1/2]^o_0$	764.2
$6p[5/2]_2-6s[3/2]^o_1$	992.3
$6p[1/2]_0-6s[3/2]^o_1$	828.0
$6p[1/2]_1-6s[3/2]^o_2$	980.0
$6p[5/2]_3-6s[3/2]^o_2$	881.9

The optical scheme of measurements is shown in Fig. 2. Broadband light source (*1*) emitting pulses of nearly trapezoidal shape (the 'plateau' duration was ~15 μs) was used for absorption probing. The output radiation of the source was collimated into a beam of diameter 50 mm, passed through measurement chamber (*3*) with a mixture under study, and was focused on the entrance slit of wide-aperture monochromator (*5*) with the 600 lines mm^{-1} diffraction grating. Radiation separated by the monochromator at the required wavelength was detected with fast germanium photodiode (*6*) and a C8-13 storage oscilloscope. Radiation at the wavelength corresponding to the second diffraction order was cut-off with optical filter (*7*). The time resolution of the detection system was ~100 ns.

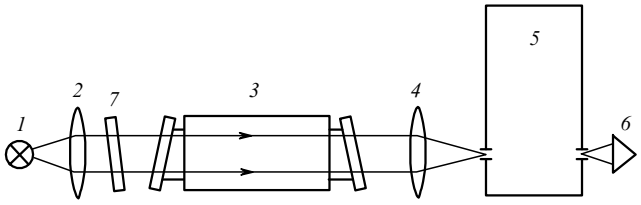

Figure 2. Optical scheme of absorption measurements: (*1*) ISI-1 pulsed light source; (*2*) collimating lens; (*3*) measurement chamber; (*4*) focusing lens; (*5*) MDR-2 wide-aperture monochromator; (*6*) FD-10GA photodetector; (*7*) KS-18 optical filter.

Most of the experiments were performed using a laser with an electron gun with a hot cathode in the Tandem laser setup (see details in Ref. [1]). The electron gun was fed by rectangular voltage pulses. The ~250-keV, 10×100-cm electron beam with the pulse duration of $3-10$ μs was injected into the measurement chamber perpendicular to its optical axis through a titanium foil of thickness 20 μm. The electron current density j was controlled and could achieve

400 mA cm^{-2}. If necessary (for example, when the probe pulse was too strongly absorbed by the medium under study), the longitudinal size of the electron beam and, correspondingly, the active-region length L could be reduced with the help of metal screens placed inside the electron gun in the electron beam. Some experiments were performed using a laser with the cold cathode of the electron gun. In this case, the current pulse was bell-shaped and its duration was ~ 2.5 μs (in the base).

The measurement chamber was made of stainless steel. Before filling with a gas under study, the chamber was pumped through a nitrogen trap down to $\sim 10^{-5}$ Torr. The rate of air leaking into the chamber did not exceed 10^{-3} Torr h^{-1}. We studied the mixtures of argon (99.998 % purity) or helium (99.995 % purity) with a small amount of xenon (99.9992 % purity).

Figure 3 shows one of the oscillograms of the probe-pulse absorption obtained on the setup with the hot cathode. Each of the oscillograms was formed by the superposition of three output signals from the photodetector on the screen of the C8-13 storage oscilloscope. Signal (*1*), detected when the probe radiation source was switched off, gives the time base (zero transmission of a signal). Signal (*2*), obtained when the probe radiation source was switched on and the electron gun was switched off, corresponds to the 100-% transmission of radiation. Signal (*3*), obtained when both the probe radiation source and the electron gun were switched on, shows the transmission of radiation in the excited medium. A comparison of signals (*2*) and (*3*) corresponding to signals at the entrance into and exit from the excited active medium allows us to determine at each instant of time the transmission coefficient at the wavelength separated by the monochromator.

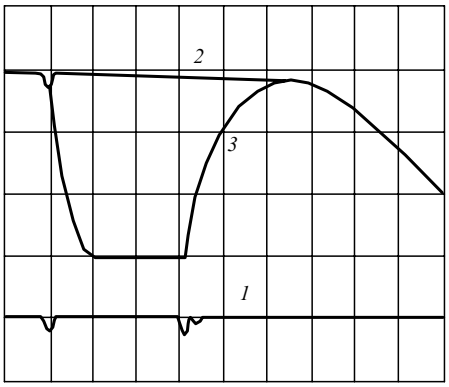

Figure 3. Oscillogram of the 828-nm probe pulse absorption in the Ar : Xe = 99 : 1 mixture at a pressure of 3 atm for the electron current density $j = 400$ mA cm^{-2} (2 μs/div time base).

The applicability of the method of absorption probing is determined to a great extent by the relation between the spectral width of the probed transition and the width of the instrumental function of the monochromator. In our case, for the width of the entrance and exit slits of the monochromator equal to ~ 0.1 mm providing the satisfactory signal-to-noise ratio in the detection system, the spectral resolution in the pressure range studied was comparable with the half-width of the optical transition. In this situation, the Bouguer – Lambert – Beer law is not fulfilled. However, it is known that, when only instrumental distortions are present, the empirical (so-called modified) Lambert – Beer law can be used [34, 35], which gives the relation between the measured transmission coefficient T and the absorption coefficient k_{ab} proportional to the concentration of the state under study:

$$\ln T^{-1} = (k_{ab}L)^{\gamma}, \tag{30}$$

where the dimensionless factor γ varies from 1 to 0.5 depending on the ratio of the half-widths of the absorption line and the instrumental function of the monochromator.

The factor γ was determined experimentally for each of the transitions studied. For the fixed parameters of a gas mixture and the pump level at some specified instant of time t_0 with respect to the onset of the electron current pulse (the coefficient k_{ab} is fixed), the Lambert – Beer law can be written as the dependence of the transmission coefficient T_0 of the probe signal on the active-region length L:

$$\ln \ln T_0^{-1} = \text{const} + \gamma \ln L. \tag{31}$$

The corresponding experimental dependences for all transitions in Table 3 in the range $T_0 = 0.15 - 0.85$ were well described by straight lines, which confirms the validity of expression (31) and permits the calculation of γ by the slope of these curves (in most cases, the coefficient γ was close to 0.5).

4. Experiment

Of four 6*s* and 6*s*′ levels of a Xe atom investigated in this paper (see Fig. 1), two are metastable and two are resonance. However, at high pressures of xenon-containing gases, spontaneous VUV radiation from excited resonance levels proves to be completely trapped, and these levels also can be treated as metastable. As a result, the depopulation of these excited states is completely determined by deactivation processes in collisions of Xe* with ground-state Xe, He, and Ar atoms.

In the Ar – Xe and He – Xe laser mixtures with a relatively low content of xenon (less than 1/50), the influence of reactions of the type

$$\text{Xe}^* + \text{Xe} \rightarrow \text{products} \tag{32}$$

and (28) on deactivation can be neglected. Then, after the end of the pump pulse and termination of recombination and relaxation processes populating the 6*s* and 6*s*′ states, the deactivation rates of these states will be determined by three-particle collisions with atoms of argon, helium, and xenon in reactions (29) and

$$\text{Xe}^* + 2\text{Ar}(2\text{He}) \rightarrow \text{ArXe}^*(\text{HeXe}^*) + \text{Ar}(\text{He}), \tag{33}$$

which are quadratic in pressure, and also in reactions

$$\text{Xe}^* + \text{Ar}(\text{He}) \rightarrow \text{Xe (other } 6s \text{ and } 6s' \text{ states)} + \text{Ar}(\text{He}), \tag{34}$$

which are linear in pressure

However, when determining the rate constants of reactions (34), one should bear in mind that the rate constants measured experimentally are, generally speaking, upper estimates because collisions between excited xenon and impurity atoms and molecules in reactions

$$Xe^* + \text{impurities} \rightarrow Xe + \text{products} \quad (35)$$

should be also taken into account. Although concentrations of impurities in gases studied in our experiments were low, the interaction of the electron beam with the inner surface of the measurement chamber can result in an uncontrollable pollution of the working volume by molecules adsorbed on the surface. Note that, because of the large interaction cross section, the contribution from reaction (35) can be in principle noticeable even at low concentrations of these uncontrollable molecular impurities.

Therefore, the concentration of excited states of the Xe atom after the completion of recombination and relaxation is described by the differential equation

$$\frac{d[Xe^*]}{dt} = -(k_{34} + k_m M)[Ar]([He])[Xe^*]$$

$$-k_{29}[Xe][Ar]([He])[Xe^*] - k_{33}[Ar]^2([He]^2)[Xe^*], \quad (36)$$

and the time dependence of the population of each of these states can written in the form

$$[Xe^*](t) = N_0 \exp(-t/\tau_d), \quad (37)$$

where

$$\tau_d^{-1} = (k_{34} + k_m M)[Ar]([He]) + k_{29}[Xe][Ar]([He])$$

$$+ k_{33}[Ar]^2([He]^2) \quad (38)$$

is the deactivation rate of the state under study; k_{29} and k_{33} are the rate constants of excimer formation in reactions (29) and (33), respectively; k_{34} is the rate constant of two-particle relaxation (34); k_m is the rate constant of quenching by impurities in reaction (34); and M is the relative concentration of the impurity in the mixture under study. Taking the logarithm of expression (30) and accounting for the exponential dependence (37) for $[Xe^*](t)$, we obtain a simple expression

$$\ln\ln T^{-1} = \text{const} - \gamma t/\tau_d \quad (39)$$

for the time dependence of the transmittance T of the probe signal in the afterglow.

Figure 4 shows typical experimental dependences of $\ln\ln T^{-1}$ on time, which were obtained for the $^3P_2$ level in the He : Xe = 75 : 1 mixture by processing by points the trailing edges of oscillograms of the 881.9-nm probe-beam absorption pulses (the time was measured from the end of the electron-beam pulse). One can see that, within ~ 1 μs after the end of the electron current, experimental points lie on a straight line with good accuracy. This circumstance confirms the applicability of the modified Lambert–Beer law in this case and the validity of the model used. Similar dependences were obtained for all xenon levels studied in Ar–Xe and He–Xe mixtures with the ratios of components from 50 : 1 to 1000 : 1 in the pressure range from 1 to 3–4 atm. In accordance with (39), the slope of the straight lines obtained, taking into account the factor γ, gives the deactivation rate τ_d^{-1} of the state studied under the corresponding experimental conditions.

To determine the contribution from one or another plasma-chemical reaction to the deactivation rate for each

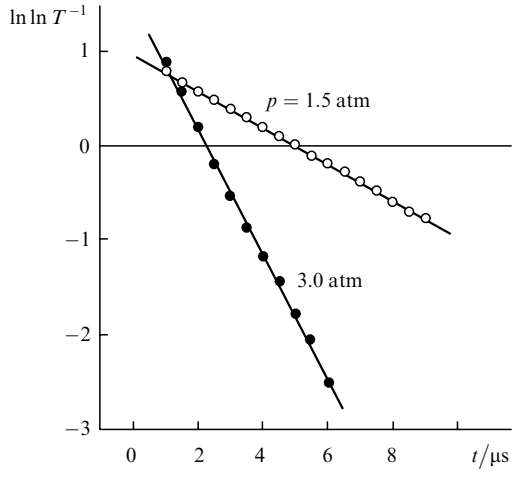

Figure 4. Time dependences of $\ln\ln T^{-1}$ for the $6s[3/2]_2^o$ level (881.9 nm) at the trailing edge of an absorption pulse in the mixture He : Xe = 75 : 1 at different pressures.

Ar–Xe and He–Xe mixture, it is convenient to represent the experimental values of τ_d^{-1} obtained this way as the dependence of the quantity τ_d^{-1} [buffer gas]$^{-1}$ on the buffer gas concentration, i.e., as the dependence of the deactivation rate reduced to the argon or helium concentration (such typical dependences for quenching of the $^3P_2$ level in helium mixtures are shown in Fig. 5). In accordance with the linearity of dependences

$$\tau_d^{-1}[Ar]^{-1}([He]^{-1}) = (\delta k_{29} + k_{33})[Ar]([He])$$

$$+ (k_{34} + k_m M) \quad (40)$$

[$\delta = [Xe]/([Xe] + [Ar]([He])$] is the relative concentration of xenon in the mixture) predicted in (38), experimental points lie on straight lines. The points of intersection of these straight lines with the ordinate axis give the rate constants for reactions (34), which are linear in the buffer-gas concentration [reactions (11)–(14) in Table 1 and reactions (23)–(26) in Table 2], while the slopes of the straight lines give the numerical values for the expression

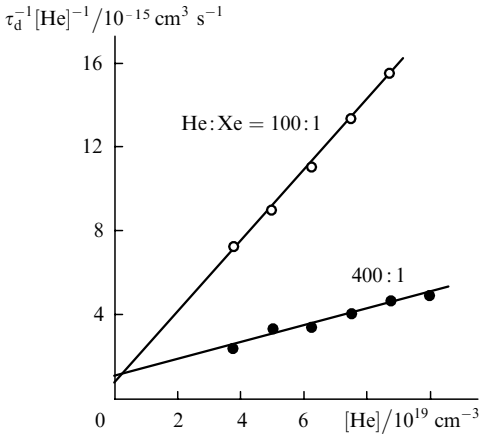

Figure 5. Dependences of the reduced deactivation rate $\tau_d^{-1}[He]^{-1}$ for the $6s[3/2]_2^o$ level on the helium concentration in the He–Xe mixtures of different compositions.

$$\delta k_{29} + k_{33}, \tag{41}$$

which is the superposition of the rate constants for three-particle reactions (29) and (33).

As mentioned above, the rate constants obtained for reactions (34) are, generally speaking, the upper estimates with the accuracy to the unknown value $k_m M$. Such is indeed the case for the results obtained in our first papers [16, 17] in a series of publications in this field. However, in further experiments we paid special attention to the purity of gases. We always used only pure gases, and the measurement chamber was evacuated before each experiment through a nitrogen trap down to $\sim 10^{-5}$ Torr. It is important that, by accumulating the required statistics, we performed the minimal number of 'shots' in each experimental series, providing the conditions under which the electron beam did not produce any noticeable amounts of foreign impurities in the active medium. That is why we believe that the rate constants of reactions presented in this paper are close to their real values.

The rate constants of three-particle processes, which are quadratic in pressure, were separated in three stages. At the first stage, we plotted the dependences of the deactivation rates τ_d^{-1} on the xenon concentration for xenon levels measured in mixtures of different compositions at several fixed pressures [i.e., at fixed concentrations of the buffer gas, because the partial pressure of argon (or helium) in mixtures with a low relative concentration of xenon virtually coincides with the total pressure of the mixture] (Fig. 6). In this case, experimental points were well approximated by straight lines, according to (38). The slopes of the straight lines gave the value of the product k_{29}[Ar] (or k_{29}[He]) for each concentration of the buffer gas.

At the second stage, we plotted the dependences of the above products on the buffer-gas concentration (Fig. 7). The dependences are well described by straight lines passing through the coordinate origin. The slopes of these straight lines give the rate constants k_{29} for reactions (3)–(6) in Table 1 and reactions (15)–(18) in Table 2.

At the third stage, we subtracted the product δk_{29} from superposition (41) for each mixture studied, which allowed us to find the rate constants k_{33} for reactions (7)–(10) presented in Table 1 and reactions (19)–(22) presented in Table 2. Because the values of k_{33} estimated in this way proved to be zero within the experimental accuracy of our measurements [$(1-2)\times10^{-35}$ cm^6 s^{-1}] in all cases, the rate constants k_{33} presented in Tables 1 and 2 are upper estimates.

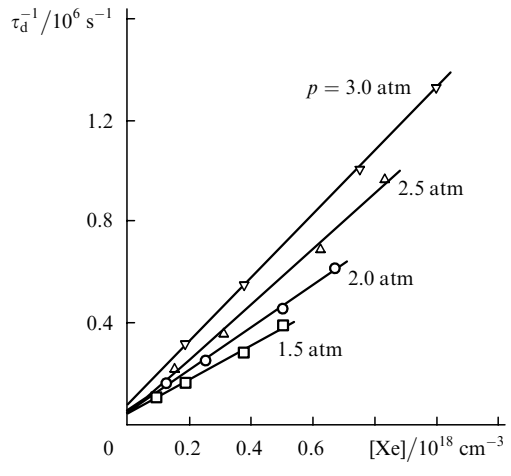

Figure 6. Dependences of the deactivation rates τ_d^{-1} of the $6s[3/2]_2^o$ level on the xenon concentration in the He–Xe mixture at different pressures.

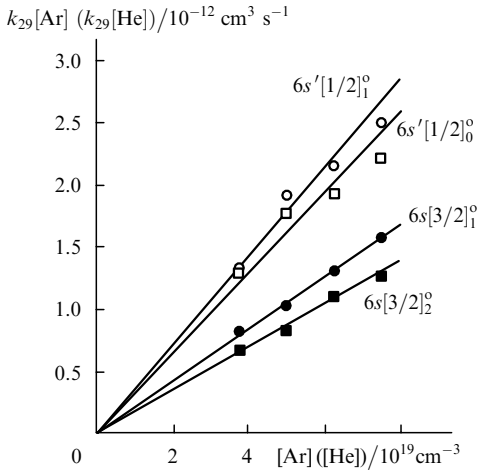

Figure 7. Dependences of k_{29} on the argon (open circles and squares) or helium (dark circles and squares) concentration for different levels of xenon.

5. Discussion of the results of measurements

We analysed the oscillograms of absorption pulses assuming that the tails of oscillograms were processed after the end of all recombination and relaxation processes, which cause the initial population of the level from higher-lying states. At the same time, we should bear in mind that, if the characteristic deactivation time of some of the higher-lying states is longer than the deactivation time of the level under study, then, irrespective of the method used, the measurements will be related to the lowest of the processes considered. However, because the rates of collisional deactivation of the 6*s* and 6*s*′ states in the Ar–Xe and He–Xe mixtures measured in our experiments (Table 1 and 2, respectively) increase with increasing the level energy and are substantially lower than these rates for the 6*p* levels reported in the literature, we conclude that the above kinetic model is valid and the results of our study are correct.

Processes of associative ionisation

$$\mathrm{Xe}(6s, 6s') + \mathrm{Xe}(6s, 6s') \rightarrow \mathrm{Xe}^+ + \mathrm{Xe} + e, \tag{42}$$

can increase the deactivation times observed in experiments. We explained by these processes the existence of quite high small-signal gains in the Ar–Xe active medium at $p \sim 1$ atm after the end of the pump pulse [36]. In experiments described here, this was manifested in the fact that experimental points in plots for the reduced deactivation rates (of Fig. 5 type) at low mixture pressures lay below straight lines drawn through the majority of points at higher pressures. The results of measurements under such experimental conditions were, naturally, discarded in the construction of the dependences discussed in section 4 and in the determination of the rate constants.

By comparing our experimental results with the data obtained by other authors beginning from the less studied

He–Xe mixture, note once more that, when the specific state of a xenon atom is not indicated in a paper, it is reasonable to assign the presented rate constant of the corresponding reaction to the lower metastable $^3P_2$ state. The rate constant of three-particle excimer-formation reaction (18) that we obtained for this state in the He–Xe mixture (Table 2) is in satisfactory agreement with such 'assigned' values of this rate constant reported in Ref. [20]. For other states, the rate constants of such reactions in the He–Xe mixture were measured probably for the first time [reactions (15)–(17)]. As mentioned above, we observed a monotonic increase in the rate constants with increasing the level energy.

We also estimated for the first time the rate constants of the excimer-formation reactions (19)–(22). Note that anomalously small values of these rate constants [$(1-2)\times10^{-35}$ cm^6 s^{-1}] presented in Table 2 are determined, as mentioned above, by experimental errors and are in fact upper estimates.

At present no data on the rate constants of reactions (25) and (26) are available in the literature. At the same time, we see (Table 2) that the rate constants for reactions (23) and (24) reported in Ref. [15] are almost two orders of magnitude higher than those obtained in our paper. However, the rate constants determined indirectly from analysis of the deactivation of the $6p$ levels in Ref. [15] cannot be considered reliable. Indeed, let us compare the numerical estimates of the characteristic relaxation times based on the experimental data obtained in Ref. [15] with our experimental values.

Because the relative contribution of two-particle reactions (23) and (24) to the deactivation of a specific level increases as the total pressure of the mixture and the relative concentration of Xe in it decrease, we will make comparison for the He : Xe = 1000 : 1 mixture (the lowest content of Xe) at a pressure of 1.5 atm (the lowest pressure in this series of experiments). According to our measurements, then lifetimes τ_d of the resonance ($^1P_1$) and metastable ($^3P_0$) states were ~ 8 and 10 μs, respectively. At the same time, the calculation based on the data presented in Ref. [15] gives $\tau_d = 0.2$ and 0.05 μs, respectively. This discrepancy is too large and cannot be explained by possible inaccuracies of our measurements. Therefore, we can claim that the rate constants of reactions (23) and (24) were also measured for the first time in our paper.

For the Ar–Xe mixtures studied in more detail, we measured in this paper for the first time the rate constant of reaction (4) and made the upper estimates of the rate constants for reactions (7)–(9). We can probably consider that our measurements of the rate constants of reactions (10) and (11) were also performed for the first time because the discrepancy between our data and the results obtained in Ref. [23] for reaction (10) and Refs [15, 32] for reaction (11) is too large. As in the case of reactions (23) and (24) in the He–Xe mixture, this discrepancy cannot be explained by possible inaccuracies of our measurements and casts doubts on the correctness of indirect methods for determining the rate constants from the experimental data array used in Ref. [15, 32].

Among other reactions, we point out that our data are in satisfactory agreement with data [31] for reaction (5), data [20, 21, 31] for reaction (6), and data [23, 33] for reaction (14). The agreement with data [30, 31] for reaction (3) is somewhat worse.

Note that, as a rule, the rate constants of reactions measured in our experiments were lower than those reported in the literature. Considering this circumstance, one should bear in mind that measurements of the deactivation rates are in principle upper estimates because any uncontrollable processes, for example, the production of undesirable impurities during experiments can only decrease but not increase the lifetime of the state under study. For this reason, the lowest of the measured values of the rate constant is usually the most reliable.

Completing the discussion of Tables 1 and 2, we consider the possible reason for anomalously small values of the rate constants for excimer-formation reactions of type (33). Note that, because of a small depth of the potential well of heteronuclear excimers HeXe* and ArXe* (~ 0.07 eV for ArXe* [23] and even smaller for HeXe*) in mixtures with a high content of helium or argon, the population of the Xe* states should depend substantially on reactions

$$\mathrm{ArXe^*(HeXe^*) + Ar(He) \rightarrow Xe^* + 2Ar(2He)}, \tag{43}$$

which are reverse to reactions (33). Apart from reactions (43), the HeXe* and ArXe* excimers can be also decomposed due to spontaneous radiative decay

$$\mathrm{ArXe^*(HeXe^*) \rightarrow products} + h\nu \tag{44}$$

and in collisions with xenon atoms in reactions

$$\mathrm{ArXe^*(HeXe^*) + Xe \rightarrow Xe_2^* + Ar(He)}. \tag{45}$$

In this case, the populations of the excited Xe and heteronuclear excimers are described by (for the example of 'helium' mixtures) by the set of equations

$$\frac{\mathrm{d[Xe^*]}}{\mathrm{d}t} = -k_{34}[\mathrm{He}][\mathrm{Xe^*}] - k_{29}[\mathrm{Xe}][\mathrm{He}][\mathrm{Xe^*}]$$

$$- k_{33}[\mathrm{He}]^2[\mathrm{Xe^*}] + k_{43}[\mathrm{He}][\mathrm{HeXe^*}], \tag{46}$$

$$\frac{\mathrm{d[HeXe^*]}}{\mathrm{d}t} = -k_{43}[\mathrm{He}][\mathrm{HeXe^*}] - k_{45}[\mathrm{Xe}][\mathrm{HeXe^*}]$$

$$- \frac{1}{\tau_{44}}[\mathrm{HeXe^*}] + k_{33}[\mathrm{He}]^2[\mathrm{Xe^*}]. \tag{47}$$

When the characteristic rates of excimer formation considerably exceed the rates of other reactions, the quasi-stationary relation between the concentrations of Xe* and HeXe* is established in active media,

$$\frac{[\mathrm{HeXe^*}]}{[\mathrm{Xe^*}]} = \frac{k_{33}}{k_{43}[\mathrm{He}] + k_{45}[\mathrm{Xe}] + 1/\tau_{44}}[\mathrm{He}]^2, \tag{48}$$

and the concentration of excited Xe satisfies the differential equation

$$\frac{\mathrm{d[Xe^*]}}{\mathrm{d}t} = -(k_{34}[\mathrm{He}] + k_{29}[\mathrm{Xe}][\mathrm{He}]$$

$$+ \frac{k_{33}k_{45}[\mathrm{Xe}] + k_{33}1/\tau_{44}}{k_{43}[\mathrm{He}] + k_{45}[\mathrm{Xe}] + 1/\tau_{44}}[\mathrm{He}]^2)[\mathrm{Xe^*}] \tag{49}$$

with the characteristic deactivation rate

$$\tau_{\rm d}^{-1} = k_{34}[{\rm He}] + k_{29}[{\rm Xe}][{\rm He}] + k_{33}\frac{k_{45}[{\rm Xe}] + 1/\tau_{44}}{k_{43}[{\rm He}] + k_{45}[{\rm Xe}] + 1/\tau_{44}}[{\rm He}]^2. \quad (50)$$

In the case of a deep potential well of the excimer when

$$k_{43}[{\rm He}] \ll k_{45}[{\rm Xe}] + 1/\tau_{44}, \quad (51)$$

the expression for the deactivation rate will contain three components corresponding to reactions (34), (29), and (33):

$$\tau_{\rm d}^{-1} = k_{34}[{\rm He}] + k_{29}[{\rm Xe}][{\rm He}] + k_{33}[{\rm He}]^2. \quad (52)$$

However, assuming reasonably that in the case of a small depth of the potential well of the $HeXe^*$ excimer, the rate of reaction (43) considerably exceeds the rates of reactions (45) and (44),

$$k_{43}[{\rm He}] \gg k_{45}[{\rm Xe}] + 1/\tau_{44}, \quad (53)$$

we obtain the expression

$$\tau_{\rm d}^{-1} = \left(k_{34} + \frac{k_{33}}{k_{43}\tau_{44}}\right)[{\rm He}] + \left(k_{29} + \frac{k_{33}k_{45}}{k_{43}}\right)[{\rm Xe}][{\rm He}] \quad (54)$$

for the deactivation rate. Therefore, if the probability of decomposition of the $HeXe^*$ complex in reaction (43) into initial components Xe^* and He considerably exceeds the probability of relaxation to lower states in reactions (45) and (44), then components proportional to the squared buffer-gas concentration should be absent in the expression for the deactivation rate.

In the general case (50), the expression for the reduced deactivation rate $\tau_{\rm d}^{-1}[{\rm He}]^{-1}$ is not linear with respect to the buffer-gas concentration, which contradicts to our experimental data. In the case (54), however, the expression for the reduced deactivation rate becomes linearly dependent on the helium concentration, as we observed in our experiments:

$$\tau_{\rm d}^{-1}[{\rm He}]^{-1} = \left(k_{34} + \frac{k_{33}}{k_{43}\tau_{44}}\right) + \delta\left(k_{29} + \frac{k_{33}k_{45}}{k_{43}}\right)[{\rm He}]. \quad (55)$$

6. Conclusions

We have measured the rate constants for 24 plasma-chemical reactions responsible for collisional deactivation of the 6*s* and 6*s*′ states of the Xe atom and involved in processes of population of the excited states of the working gas in the Ar–Xe, He–Xe, and He–Ar–Xe laser media. By the time of the statement of this work, these reactions were not adequately studied and required additional investigations, while 17 of them have been studied in our paper for the first time.

The measurements were performed by the method of absorption probing using a broadband ISI-1 radiation source to illuminate mixtures excited by a fast-electron beam. On the one hand, the use of a rather extended electron beam (the length of the excited volume was $L = 1$ m) for excitation of active media allowed us to have the required optical density at the atomic transitions for moderate pump levels. Thus, once the electron beam was switched off, after the time sufficient for a full completion of dissociative recombination and following relaxation of Xe to lower excited states, the required dynamic range was provided for the reliable detection of the time dependence of the transmission coefficient for the probe signal. On the other hand, the use of a uniquely bright ISI-1 radiation source developed in Russia [37], which is usually called the Podmoshenskii source, provided a quite satisfactory signal-to-noise ratio in the detection system of a high-voltage setup with a rather high level of the electromagnetic noise.

By processing our experimental data, we found that the components proportional to the square of the buffer-gas concentration were zero within the accuracy of measurements, and the deactivation rate can be written in the form

$$\tau_{\rm d}^{-1} = k_{\rm db}[{\rm He}] + k_{\rm tr}[{\rm Xe}][{\rm He}]. \quad (56)$$

Analysis of kinetic processes showed that the expression obtained for $\tau_{\rm d}^{-1}$ does not suggest that processes of type (33) have low rates, and the form of this expression can be explained by the influence of very fast reverse reactions of type (43). In this case, reactions (33), (43), and accompanying reactions of substitution (45) and radiative decay of heteronuclear excimers (44) can make a certain contribution to the components proportional to the buffer-gas concentration, and the 'effective' rate constants for such two-particle and three-particle deactivation reactions will have the form

$$k_{\rm db} = k_{34} + \frac{k_{33}}{k_{43}\tau_{44}}, \quad k_{\rm tr} = k_{29} + \frac{k_{33}k_{45}}{k_{43}}. \quad (57)$$

Therefore, the rate constants of reactions (29) and (34) that we (and other authors) obtained are in fact some upper estimates made with the accuracy to unknown products

$$\frac{k_{33}k_{45}}{k_{43}}, \quad \frac{k_{33}}{k_{43}\tau_{44}}. \quad (58)$$

All the measurement methods used at present, which are based on the analysis of the time dependence of excited Xe (and on the measurement of the time dependence of the concentration of heteronuclear excimers, which is possible in principle), do not allow one to determine contributions from each of the plasma-chemical reactions to the deactivation rate. However, all these reactions are automatically taken into account in the simulation of kinetic processes by describing concentrations of excited Xe by phenomenological equations

$$\frac{{\rm d}[{\rm Xe}^*]}{{\rm d}t} = -k_{\rm db}[{\rm He}][{\rm Xe}^*] - k_{\rm tr}[{\rm Xe}][{\rm He}][{\rm Xe}^*] \quad (59)$$

and assuming that the rate constants obtained in experiments characterise some 'generalised' two- and three-particle processes:

$$k_{29}^{\rm meas} \Rightarrow k_{\rm db}, \quad k_{34}^{\rm meas} \Rightarrow k_{\rm tr}. \quad (60)$$

Acknowledgements. The authors thank D.A. Zayarnyi and A.Yu. Chugunov for the daily collaboration and help in this work.

References

1. Kholin I.V. *Kvantovaya Elektron.*, **33**, 129 (2003) [*Quantum Electron.*, 33, 129 (2003).
2. Rhodes C.K. (Ed.) *Excimer Lasers* (New York: Springer-Verlag, 1979; Moscow: Mir, 1981).
3. Jackob G.H., in *Applied Atomic Collision Physics* Ed. by E.W. McDaniel and W. Nigan (New York: Acad. Press, 1982; Moscow: Mir, 1986) Vol. 3, pp 332–382.
4. Derzhiev V.I., Zhidkov A.G., Sereda O.V., Yakovlenko V.I. *Trudy IOFAN*, **21**, 139 (1989).
5. Ohwa M., Moratz T., Kushner M.J. *J. Appl. Lett.*, **66** (11), 5131 (1989).
6. Klopovskii K.S., Luk'yanova A.V., Rakhimov A.T., Suetin N.V. *Kvantovaya Elektron.*, **16**, 205 (1989) [*Sov. J. Quantum Electron.*, **19**, 133 (1989)].
7. Dudin A.Yu., Zayarnyi D.A., Semenova L.V., Ustinovskii N.N., Kholin I.V., Chugunov A.Yu. *Kvantovaya Elektron.*, **18**, 921 (1991) [*Sov. J. Quantum Electron.*, **21**, 833 (1991)].
8. Dudin A.Yu., Zayarnyi D.A., Semenova L.V., Ustinovskii N.N., Kholin I.V., Chugunov A.Yu. *Kvantovaya Elektron.*, **18**, 1290 (1991) [*Sov. J. Quantum Electron.*, **21**, 1172 (1991)].
9. Alford W.J., Hays G.N. *J. Appl. Phys.*, **65** (10), 3760 (1989).
10. Patterson E.L., Samlin G.E., Brannon P.J., Hurst M.J. *IEEE J. Quantum Electron.*, **26** (9), 1661 (1990).
11. Derzhiev V.I., Zhidkov A.G., Sereda O.V., Skakun V.S., Tarasenko V.F., Fedenev A.V., Yakovlenko S.I. *Kvantovaya Elektron.*, **17**, 985 (1990) [*Sov. J. Quantum Electron.*, **20**, 902 (1990)].
12. Berkeliev B.M., Dolgikh V.A., Rudoi I.G., Soroka A.M. *Pis'ma Zh. Tekh. Fiz.*, **17**, 76 (1991).
13. Alford W.J., Hays G.N., Ohwa M., Kushner M.J. *J. Appl. Phys.*, **69** (4), 1843 (1991).
14. Lawton S.A., Richards J.B., Newman L.A., Specht L., DeTemple T.A. *J. Appl. Phys.*, **50** (6), 3888 (1979).
15. Alford W.J. *J. Chem. Phys*, **96** (6), 4330 (1992).
16. Sazhina N.N., Ustinovskii N.N., Kholin I.V. *Kvantovaya Elektron.*, **18**, 1047 (1991) [*Sov. J. Quantum Electron.*, **21**, 949 (1991)].
17. Zayarnyi D.A., Semenova L.V., Ustinovskii N.N., Kholin I.V., Chugunov A.Yu. *Kvantovaya Elektron.*, **24**, 987 (1997) [*Quantum Electron.*, **27**, 957 (1997)].
18. Zayarnyi D.A., Semenova L.V., Ustinovskii N.N., Kholin I.V., Chugunov A.Yu. *Kvantovaya Elektron.*, **25**, 229 (1998) [*Quantum Electron.*, **28**, 221 (1998)].
19. Zayarnyi D.A., Semenova L.V., Ustinovskii N.N., Kholin I.V., Chugunov A.Yu. *Kvantovaya Elektron.*, **26**, 131 (1999) [*Quantum Electron.*, **29**, 131 (1999)].
20. Rice J.K., Johnson A.W. *J. Chem. Phys.*, **63** (12), 5235 (1975).
21. Gleason R.E., Bonifield T.D., Keto J.W., Walters G.K. *J. Chem. Phys*, **66** (4), 1589 (1977).
22. Atzmon R., Cheshnovsky O., Raz B., Jortner J. *Chem. Phys. Lett.*, **29** (3), 310 (1974).
23. Kolts J.H., Setser D.W. *J. Chem. Phys.*, **68** (11), 4848 (1978).
24. Tucker J.E., Wexler B.L. *IEEE J. Quantum Electron.*, **26** (9), 1647 (1990).
25. Gielkens S.W.A., Witteman W.J., Tskhai V.N., Peters P.J.M. *IEEE J. Quantum Electron.*, **34** (2), 250 (1998).
26. Kannari F., Suda A., Obara M., Fujioka T. *IEEE J. Quantum Electron.*, **19** (10), 1587 (1983).
27. Nishida N., Takashima T., Tittel F.K., Kannari F., Obara M. *J. Appl. Phys.*, **67** (9), 3932 (1990).
28. Kolts J.H., Setser D.W. *VII Winter Colloq. High Power Visible Lasers* (Park City, Utah, 1977).
29. Leichner P.K., Palmer K.F., Cook J.D., Thueneman M. *Phys. Rev. A*, **13** (5), 1787 (1976).
30. Galy J., Aouame K., Birot A., Brunet H., Millet P. *J. Phys. B*, **26** (3), 477 (1993).
31. Brunet H., Birot A., Dijols H., Galy J., Millet P., Salamero Y. *J. Phys. B*, **15** (17), 2945 (1982).
32. Laporte P., Subtil J.L., Reinunger R., Gurtler P. *Chem. Phys.*, **177** (1), 257 (1993).
33. Sewraj N., Gardou J.P., Salamero Y., Millet P. *Phys. Rev. A*, **62**, 052721 (2000).
34. Oka T. *Res. Rep. Nagaoka Tech. Coll.*, **13** (4), 207 (1977).
35. Davis C.C., McFarlane R.A. *J. Quant. Spectrosc. Radiat. Transfer*, **18**, 151 (1977).
36. Dudin A.Yu., Zayarnyi D.A., Semenova L.V., Ustinovskii N.N., Kholin I.V., Chugunov A.Yu. *Kvantovaya Elektron.*, **20**, 669 (1993) [*Quantum Electron.*, **23**, 578 (1993)].
37. Demidov M.I., Ogurtsova N.N., Podmoshenskii I.V. *Zh. Prikl. Spektr.*, **12**, 365 (1970).